



Engineered Fiber Crimp Alters Scaffold Mechanics, Cell Shape, and Strain Transfer to the Nucleus

¹Tristan P. Driscoll

²Jefferson Chang

³Ty'Quish S. Keyes

⁴Michael W. Hast, PhD

⁵Su-Jin Heo

⁶Robert L. Mauck, PhD

⁷Pen-Hsiu Grace Chao, PhD

¹University of Pennsylvania,
Departments of Orthopaedic Surgery and
Bioengineering, Philadelphia, PA, USA

²National Taiwan University, Taipei, Taiwan

³Morehouse College, Atlanta, GA, USA

⁴University of Pennsylvania,
Department of Orthopaedic Surgery,
Philadelphia, PA, USA

Introduction

Tendons and ligaments are composed of highly aligned collagen fibers that, at the micron-scale, have an intrinsically crimped micro-architecture.¹ With stretch, crimped fibers straighten, resulting in a non-linear mechanical response.^{2,3} Crimp is thus a critical structural adaptation providing function under physiologic strain⁴ and is lost with pathological conditions.⁵ When such tissues are damaged, one treatment strategy is to engineer replacement tissues using highly aligned arrays of polymer nanofibers, created by electrospinning.⁶ Recently, this technique has been further refined to generate fiber crimp by heating scaffolds to their glass-transition temperature.⁷ In our previous work, accelerated cellular infiltration was achieved by increasing scaffold porosity with inclusion of a water-soluble sacrificial poly-ethylene oxide (PEO) component.⁸ In this study, we increased scaffold crimp by increasing scaffold porosity prior to heating, thus providing increased space for scaffold crimp formation. We then probed the bulk scaffold mechanics and the micromechanical response of both the scaffold and attached cells, identifying differences that will likely regulate mechanotransduction in cells interacting with this material.

Methods

Aligned nanofibrous scaffolds were generated by electrospinning, onto a rotating mandrel, a 8.5% w/v solution of poly-L-lactide (PLLA) in HFP either alone or in combination with a second spinneret containing a 10% w/v solution of PEO in 90% ethanol. These two scaffold types (PLLA only or PLLA/PEO dual) were washed with decreasing concentrations of ethanol (to hydrate and/or remove PEO) or heated to 65° between two glass plates (to induce crimp). Dual scaffolds were washed (DW), heated and then washed (DHW), or washed and then heated (DWH). This last group (DWH) is expected to produce the highest degree of crimp, due to the increased porosity present during heating. Scaffolds (40x5mm²) were measured using a laser based device (cross-section) and tested in uniaxial tension using an Instron 5848 (n=3/ grp) with a custom cross-polarized light fixture

to measure fiber alignment.³ Linear modulus and transition strains were calculated using bi-linear fits (Matlab). Additional scaffolds (70x5mm²) were coated with fibronectin (20µg/ml), seeded with p1 bovine mesenchymal stem cells (MSCs, 100k cells), and cultured for 2 days in chemically defined media. F-Actin (phalloidin) and nuclear (DAPI) staining of cell-seeded scaffolds (n=2/grp) was performed to assess cell shape and alignment; fibers were imaged from autofluorescence. Dual scaffold groups were stained with Hoechst (nuclei) in DMEM (20 min; 37°C) then stretched (n=4/grp) in 1% increments to 8% strain using a microscope-mounted tensile device. Micro-scale Lagrangian strains were calculated from nuclear triads, and a Poisson's ratio was calculated for each triad. Nuclear deformation was quantified using the ratio of nuclear principal lengths (nuclear aspect ratio, NAR) and nuclear orientation quantified as angle of the nuclear principal axis (0-90° where 90° = fiber/stretch direction). One-way ANOVA with Tukey's post hoc (mechanics) and two-way ANOVA with Bonferroni post hoc (nuclear angle and NAR) were used to determine statistical differences between groups.

Results

Mechanical testing showed that heating or inclusion of sacrificial PEO fibers resulted in a decrease in the linear modulus (Figure 1A) and an increase in the transition strain (Figure 1B,C) with the most crimped scaffold (DWH) having the highest transition strain and yield strain (not shown) and the lowest degree of alignment (as measured by cross-polarized light, not shown). Imaging of actin/DAPI stained scaffolds (Figure 1D) showed that PLLA-only scaffolds had the least crimped fibers (red) and the most elongated cells (green) and nuclei (blue), whereas the DWH scaffolds had the most crimped fibers and the least elongated cells and nuclei, with some cells following the crimp pattern. Stretch of cell seeded scaffolds showed that all scaffolds displayed similar positive Lagrangian strains in the stretch direction (E_{11} , Figure 2A) that reached close to the applied strain, but that the DWH scaffolds displayed the least lateral compression (E_{22}), resulting in significantly lower micro-scale

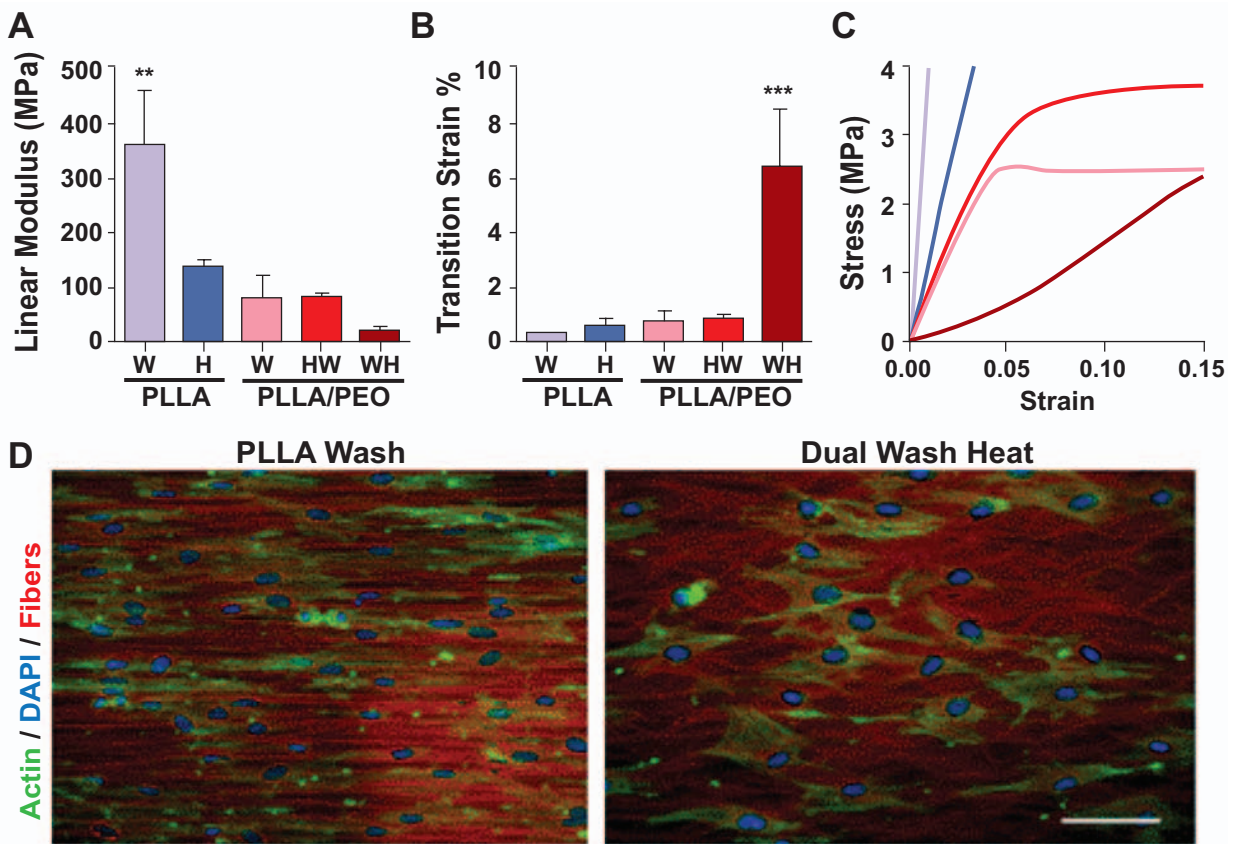


Figure 1. Tensile mechanics of PLLA and PLLA/PEO (Dual) scaffolds with various heat and wash treatments. Quantification of Linear Modulus (A) and Transition Strain (B) (mean \pm SD, ** $p < 0.01$ *** $p < 0.001$ vs. all other groups). Average stress-strain curves (C) for each group show increased toe-region in the most crimped scaffolds (DWH). Phalloidin (green) and DAPI (blue) stained scaffolds with auto-fluorescent fibers (red) for normal PLLA scaffold and crimped DWH scaffold (D). Scale bar = 75 μ m.

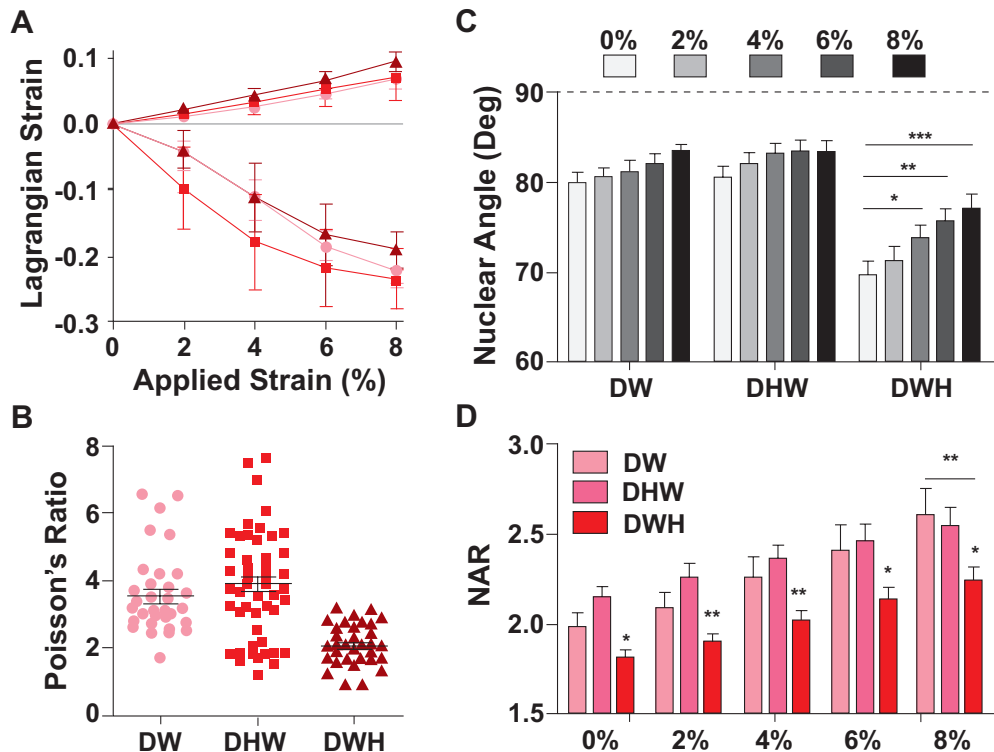


Figure 2. Lagrangian strains (mean \pm SD) in the fiber/stretch direction (A, top) and in the perpendicular direction (A, bottom) calculated from triads of MSC nuclei stained with Hoeschst and stretched on a microscope mounted device to 8% strain. Micro-scale Poisson's ratios were calculated for each triad at 8% (B). Quantification of nuclear orientation (C, where 90° = fiber/stretch direction) and nuclear aspect ratio (D, NAR) with applied strain ($n > 45$ nuclei). Mean \pm SEM, bars indicate significance between groups, * = $p < 0.05$, ** = $p < 0.01$, *** = $p < 0.001$.

Poisson's ratios (Figure 2B). These scaffolds also displayed the least aligned nuclei at 0% strain and significant nuclear reorientation at 4, 6 and 8% strain (Figure 2C), whereas other scaffolds showed only slight (not significant) reorientation. Additionally, cells on DWH scaffolds had significantly lower NAR compared to DHW scaffolds at every strain level (Figure 2D). Although all groups showed significant nuclear elongation with applied stretch, this elongation was delayed on DWH scaffolds, and did not reach DW baseline levels until 4% strain.

Discussion

The crimp structure of tendons and ligaments is vitally important for their mechanical function, but is also likely important in regulating cellular mechanotransduction within these tissues. This structure may prove important for appropriate differentiation of progenitor cells used for engineering replacement tissues and may regulate the manner in which they interpret mechanical signals they receive within the dynamically loaded host environment. Here, by including a sacrificial PEO fiber population and controlling phase transitions in fibers, we generated aligned, porous, and crimped electrospun PLLA scaffolds that display much higher transition strain than heating PLLA alone. These scaffolds also alter baseline cellular and nuclear shape and response to stretch, potentially altering cellular interpretation of these mechanical signals. Future work will focus on understanding cellular deformation and biologic response in more mature/infiltrated constructs.

Significance

Fiber crimp is an important structural and mechanical characteristic of fibrous orthopaedic tissues and likely

influences mechanotransduction within these tissues. Engineering replacement tissues will require both replication of this functional structure and understanding of its biologic influence on resident cells.

Acknowledgments

This work was supported by the NIH (T32 AR007132) the NSC (101-2221-E-002-045-MY2) and the NHRI (EX102-10019EC).

References

1. **Rigby BJ, Hirai N, Spikes JD, et al.** The Mechanical Properties of Rat Tail Tendon. *J. Gen. Physiol.* 43, 265–283 (1959).
2. **Diamant J, Keller A, Baer E, et al.** Collagen; Ultrastructure and Its Relation to Mechanical Properties as a Function of Ageing. *Proc. R. Soc. Lond. B Biol. Sci.* 180, 293–315 (1972).
3. **Lake SP, Miller KS, Elliott DM, et al.** Effect of fiber distribution and realignment on the nonlinear and inhomogeneous mechanical properties of human supraspinatus tendon under longitudinal tensile loading. *J. Orthop. Res.* 27, 1596–1602 (2009).
4. **Hansen KA, Weiss JA, Barton JK.** Recruitment of tendon crimp with applied tensile strain. *J. Biomech. Eng.* 124, 72–77 (2002).
5. **Gathercole LJ, Keller A.** Crimp morphology in the fibre-forming collagens. *Matrix Stuttg. Ger.* 11, 214–234 (1991).
6. **Li J, Shi R.** Stretch-induced nerve conduction deficits in guinea pig ex vivo nerve. *J. Biomech.* 40, 569–578 (2007).
7. **Surrao DC, Fan JCY, Waldman SD, et al.** A crimp-like microarchitecture improves tissue production in fibrous ligament scaffolds in response to mechanical stimuli. *Acta Biomater.* 8, 3704–3713 (2012).
8. **Baker BM, et al.** Sacrificial nanofibrous composites provide instruction without impediment and enable functional tissue formation. *Proc. Natl. Acad. Sci.* 109, 14176–14181 (2012).